ACS OMEGA

Open Access

http://pubs.acs.org/journal/acsodf

Article

An Efficient Synthesis of Novel Aminothiazolylacetamido-Substituted 3,5-Bis(arylidene)-4-piperidone Derivatives and Their Cytotoxicity Studies

Thangaiyan Suresh, Dhatchana Moorthy Nachiappan, G. Karthikeyan, Vijayaparthasarathi Vijayakumar, Jerry P Jasinski, and Sundaramoorthy Sarveswari*

Cite This: *ACS Omega* 2024, 9, 29244−29251

Read Online

ACCESS | Metrics & More | Article Recommendations | Supporting Information

ABSTRACT: The expansion of 3,5-bis(arylidene)-4-piperidone derivatives with heterocyclic compounds such as 1,3-thiazole should take into account this correlation. The synthesized aminothiazolylacetamido-substituted 3,5-bis(arylidene)-4-piperidone derivatives **3a−j** were found to have GI_{50} values in the range of 0.15−0.28 μM against HeLa and HCT116 cancer cell lines. *In silico* docking studies confirmed that the proteasome inhibition mechanism involves a nucleophilic attack from the N-terminal threonine residue of the β-subunits to the C═O group of compounds. A C═O group of amide was able to interact with the NH group of the alanine residue and the **5g** NH group of amino thiazole, along with an OH group of the serine residue. These results strongly suggest that the synthesized compounds could be a potential candidate inhibitor of the 20S proteasome. These molecules have the potential to be developed as cytotoxic and anticancer agents, as revealed by this study.

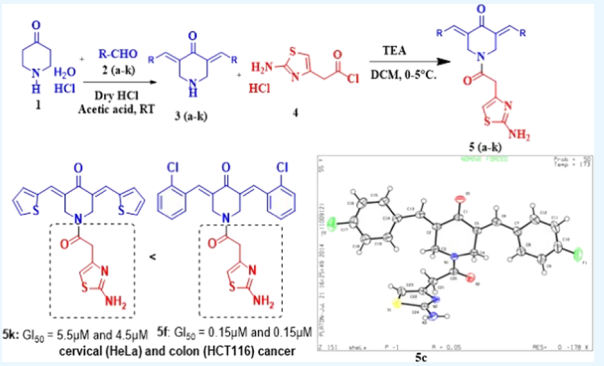

1. INTRODUCTION

Nearly 9.7 million deaths were caused by cancer in 2022, making it the primary cause of death worldwide. The number of new cancer cases is estimated to be 20 million. The most common cancers are breast, lung, colon, rectum, and prostate cancers. Colon cancer is the third most common cancer and the second most deadly. Cervical cancer ranks eighth among the most common cancers globally and ninth among the leading causes of cancer death.[1] Cancer develops within your colon (large intestine), which is the long tube that assists in transporting digested food to the rectum and out of your body. Certain polyps or growths in the inner lining of your colon can lead to colon cancer. The development of cervical cancer occurs slowly in a female's cervix over time, beginning with the appearance of abnormal cells in the cervical tissue. The growth and spread of cancer cells deeper into the cervix and surrounding areas occurs later on.

Cancer is treated through surgery, radiation, medications, and other therapies. The use of chemotherapy medication often results in the death of cells that grow and divide rapidly. The small-molecule targeted therapy helps treat cancer by interfering with specific proteins that help tumors grow and spread throughout the body shrink a cancer or stop its progression. By learning more about cancer-causing DNA changes and proteins, researchers are better equipped to create treatments that target these proteins. The proteasome pathway has an important role in apoptosis,[2,3] cell growth and proliferation,[4] DNA repair,[5] unfolded protein,[6] and immune system.[7] This pathway is a regulated process for the degradation of intracellular proteins and homeostasis of both normal and cancer cells.[8] Curcumin is an active principle with two α,β-unsaturated diketo function flanked by 4-hydroxy-3-methoxyphenyl groups, obtained from the perennial herb *Curcuma longa* which exhibits anticancer.[9] Curcumin inhibits the proteasome activity in human colon cancer cells in vitro and in vivo.[10] Based on the structure−activity relationship (SAR) studies, attempts have been made to produce curcumin analogues with improved potencies while retaining their low toxicity. In order to produce such analogues, molecular modifications have been made in the structure of curcumin at the aryl ring, β-diketo function and the two conjugated α,β-unsaturated keto function (Figure 1).

The curcumin synthetically modified to Chalcone derivative of 3,5-bis(4-boronic acid-benzylidene)-1-methyl-piperidin-4-one exhibits potent anticancer activity through inhibition of the Proteasome.[11] Chalcone-based proteasome inhibiting

Received: January 2, 2024
Revised: June 8, 2024
Accepted: June 12, 2024
Published: June 26, 2024

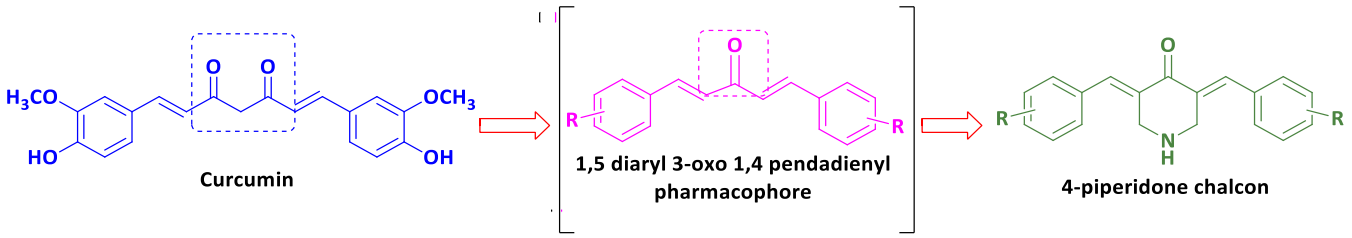

Figure 1. Modification of curcumin β-diketone to mono carbonyl moiety.

Scheme 1. Synthesis of 5(a−k)[a]

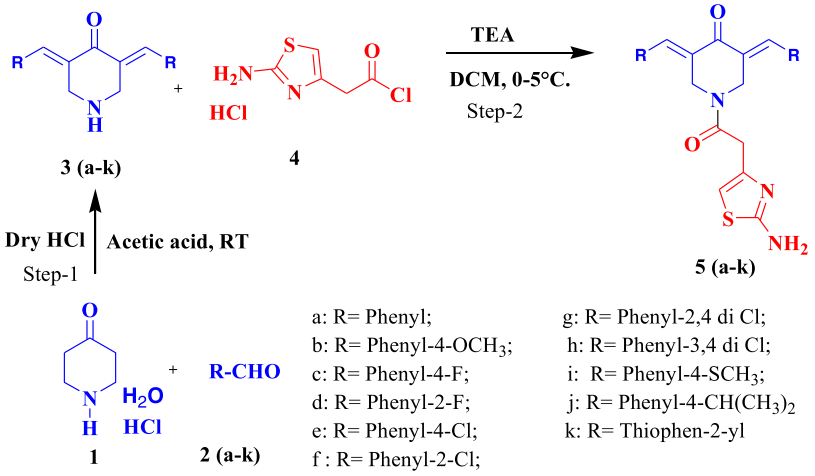

[a]Reagents and conditions: **Step-1**: arylaldehydes, dry HCl, acetic acid, RT, 30 min; **Step-2**: (2-amino-thiazol-4-yl)-acetyl chloride hydrochloride, triethylamine (TEA), dichloro methane, 0−5 °C.

nature of the amino acid portion of the molecule confers specificity toward catalytic activities of the 20S proteasome.[12] Docking studies were conducted against EGFR tyrosine kinase, a potential target for anticancer agents of 3,5-bis(substituted benzylidene)-1-ethylpiperidin-4-one analogues.[13] Many analogues with 3,5-bis(arylidene)-4-piperidone (BAP) pharmacophore were reported to inhibit the catalytic sites of 20S proteasome.[14] The BAP pharmacophore offers the possibility of substitution with various atoms on the diaryl ring and on the piperidone nitrogen atom. Structure−activity studies with various analogues of BAP showed that the arylidene piperidone pharmacophore interacts with the primary target, while the nature of the substituent on the aryl ring influences the bioactivity. It was reported that the conjugated arylidene keto functional group is the primary binding site. The *N*-acryloyl group was intercalated with a secondary binding site to increase the potency.[15,16] The aryl substitutions were chosen by altering the hydrogen bonding and hydrophobic properties. Among the various atoms in the diaryl ring, the *o*- or *p*-fluorinated phenyl group exhibited promising antiproliferative activity in a variety of cancer cells.[17,18]

The SAR study of cytotoxic BAP and related *N*-Acryloyl analogues clearly shows that electronic parameters are the most important factor influencing cytotoxicity.[12,16] The future expansion of BAP derivatives with heterocyclic compounds should take this correlation into account. 1,3-Thiazole is one of the most important scaffolds in heterocyclic chemistry, and drug design and discovery indicated that the biologically active thiazole derivatives have been more frequently introduced as chemotherapeutic agents (antibacterial, antifungal, antitubercular, antiviral, anticancer, and antiparasitic).[19] Thiazole-based compounds may be useful as inhibitors of multiple enzyme target inhibitors or some other metabolic pathways.[20,21] They are the most effective anticancer agent against the MCF-7 human breast adenocarcinoma and NIH/3T3 mouse embryonic fibroblast cell lines.[22] New derivatives of thiazole were designed and synthesized as EGFR inhibitors affecting both MCF-7 and HepG2 cancer cell lines.[23−25] The results recommended that 1,3-thiazole is one of the most important therapeutic sites.[26−31] Antibacterial,[32] antitubercular,[33] antiviral,[34] and anticancer[35] activities are among the therapeutic areas where 2-amino thiazole is an important scaffold. New 2-amino thiazole scaffolds are phosphodiesterase type 5 regulators and COX-1/COX-2 inhibitors.[36] 2-Amino thiazole analogues exhibited their potent and selective nanomolar inhibitory activity against a wide range of human cancerous cell lines, such as breast, leukemia, lung, colon, CNS, melanoma, ovarian, renal, and prostate.[37] The *N*-acryloyl analogue compounds in series are predicted to have a significant increase in cytotoxicity over the corresponding secondary amines of 3,5-bis(benzylidene)-4-piperidone.[16] In order to extend the *N*-acryloyl analogue and create a new *N*-acetamide chain, 2-amino thiazole was used in this study.

2. RESULTS AND DISCUSSION

Chemistry. The Claisen−Schmidt condensation was applied to synthesize a series of 3,5-bis(arylidene)-piperidin-4-ones. Room-temperature stirring of 2 equiv of benzaldehyde with 1 equiva of 4-piperidone hydrochloride monohydrate in the acetic acid medium afforded compounds **3a−k**. 3,5-Bis(arylidene)-piperidin-4-one derivatives (BAP) **3(a−k)** was treated with (2-aminothiazol-4-yl)-acetyl chloride (**4**) in the

https://doi.org/10.1021/acsomega.4c00039
ACS Omega 2024, 9, 29244−29251

presence of base. To prove the generality of the reaction, the procedure was repeated with (**3b−k**) to get (**5b−k**) (Scheme 1, Table 1). The synthesized compounds were characterized

Table 1

compound no	R	temp (°C)	yield (g)
5a	phenyl	0−5	3.30
5b	phenyl-4-OCH_3	0−5	3.40
5c	phenyl-4-F	0−5	3.24
5d	phenyl-2-F	0−5	3.38
5e	phenyl-4-Cl	0−5	3.20
5f	phenyl-2-Cl	0−5	3.50
5g	phenyl-2,4 di Cl	0−5	3.70
5h	phenyl-3,4 di Cl	0−5	4.20
5i	phenyl-4-SCH_3	0−5	3.70
5j	phenyl-4-$CH(CH_3)_2$	0−5	3.90
5k	thiophen-2-yl	0−5	2.90

using ^{1}H NMR, ^{13}C NMR, IR, and mass spectral analysis. The crystal structure of compound **5c** (Figure 2) and also the solved crystallographic data are given in Tables 2 and 3.

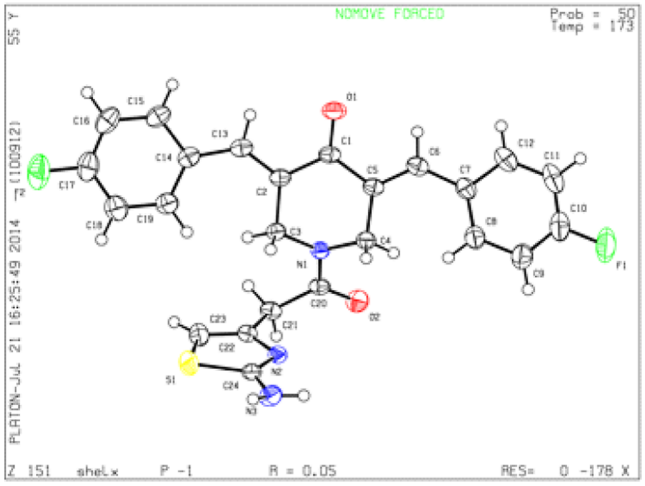

Figure 2. ORTEP of compound **5c**.

Biology. *Anticancer Activity.* The classification of molecular docking into covalent and noncovalent docking depends on whether there is an implicit bond between the target and the ligand. The noncovalent interactions that occur during docking between the target and the ligand include hydrogen bonding, Van der Waals, and electrostatic interactions. Covalent docking involves the establishment of an implicit bond between the target and the ligand during docking calculations.[38] The docked molecules were evaluated by using criteria such as binding affinity scores and the detection of significant hydrogen bonds and aromatic interactions. In yeast and mammals, each of the three proteolytic subunits presents differences when binding to substrates and activity performed: β1 subunit presents "caspase-like" (C-L) or "post acidic" (PA) activity and cleaves peptide bonds after acidic amino acids; β2 subunit has "trypsin-like" (T-L) activity, and cleaves peptide basic amino acids; β5 subunit has "chymotrypsin-like" (CT-L) activity and acts after neutral amino acids.[38] The preliminary molecular docking studies were performed for the synthesized analogues with the crystal structure of β5 subunit of the 20S proteasome using the AutoDock 4.2 software.[39,40] The model

Table 2. Crystal Data and Structure Refinement for 5c

empirical formula	$C_{24}H_{19}F_2N_3O_2S$
formula weight	451.48
temperature	173(2) K
wavelength	0.71073 Å
crystal system	triclinic
space group	$P\bar{1}$
unit cell dimensions	a = 8.2508(4) Å = 74.738(5)°
	b = 11.4354(6) Å = 84.005(4)°
	c = 11.8685(6) Å = 83.120(4)°
volume	1069.43(10) Å^3
Z	2
density (calculated)	1.402 Mg/m^3
absorption coefficient	0.196 mm^{-1}
F(000)	468
crystal size	0.39 × 0.31 × 0.17 mm^3
Theta range for data collection	2.962 to 32.870°
index ranges	$-12 \le h \le 12$, $-16 \le k \le 17$, $-17 \le l \le 17$
reflections collected	34 779
Independent reflections	7413 [R(int) = 0.0342]
completeness to θ = 25.500°	99.7%
absorption correction	semiempirical from equivalents
max. and min. transmission	1.00000 and 0.86396
refinement method	full-matrix least-squares on F2
data/restraints/parameters	7413/0/297
coodness-of-fit on F2	1.024
final R indices [$I > 2\sigma(I)$]	$R1$ = 0.0462, w$R2$ = 0.1131
R indices (all data)	$R1$ = 0.0650, w$R2$ = 0.1258
extinction coefficient	n/a
largest diff. peak and hole	0.411 and −0.475 Å^{-3}

of the predicted binding modes of compounds **5f** and **5g** into the β5 (blue)/β6 (white) active site of the 20S proteasome is shown in Figure 3; key hydrogen bonds between the inhibitor and protein are shown as red dashed lines. The docking studies revealed that the chloro-substituted compounds **5e** to **5h** showed strong binding free energies of −8.43, −8.80, −9.12, and −8.49 kcal/mol, respectively (Table 4). The chloro-substituted derivatives **5f** and **5g** showed the highest free energy of binding. Thus, it may be possible that inhibition of β5 (K chain) of 20S proteasome by compounds **5f** and **5g** is through hydrogen bonding interaction between the C═O group of piperidone ring with the HO group of THR-1 (Threonine) residue and the NH group of GLY-47 (Glycine) residue. Another C═O group of amide interacted with the NH group of the ALA-49 (alanine) residue, and the **5g** NH group of amino thiazole interacted with an OH group of the SER-96 (Serine) residue. These results strongly suggest that the synthesized compounds **5f−5h** could be potential candidate inhibitors of the 20S proteasome. *In silico* docking studies confirmed that the proteasome inhibition mechanism involves a nucleophilic attack from the N-terminal threonine residue of the β-subunits to the C═O group of compounds.

Bortezomib, carfilzomib, and ixazomib are three drugs currently on the market after extensive research in proteasome inhibitors. Proteasome inhibitor Bortezomib was used as a positive control. All synthesized compounds **5a−k** were evaluated for growth inhibition in cervical (HeLa) and human colon (HCT116) cancer cell lines. The GI_{50} values determined by the SRB cell viability assay in HeLa and HCT116 cells are shown in Table 5. The anticancer spectrum of the synthesized chalcones remains the same irrespective of

https://doi.org/10.1021/acsomega.4c00039
ACS Omega 2024, 9, 29244−29251

Table 3. Hydrogen Bonding Interactions of Compound 5c [Å and deg][a]

D−H···A	d(D−H)	d(H···A)	d(D···A)	<(DHA)
C(9)-H(9A)···F(1)#1	0.95	2.47	3.310(2)	147.3
C(21)-H(21A)···O(1)#2	0.99	2.49	3.2166(15)	130.3
N(3)-H(3N1)···N(2)#3	0.907(19)	2.18(2)	3.0895(17)	178.0(17)
N(3)-H(3N2)···O(2)#4	0.844(19)	2.149(19)	2.9636(15)	162.2(17)

[a]Symmetry transformations used to generate equivalent atoms. #1 $-x+1, -y, -z$. #2 $-x+1, -y+1, -z+1$. #3 $-x+2, -y, -z+1$. #4 $x+1, y, z$.

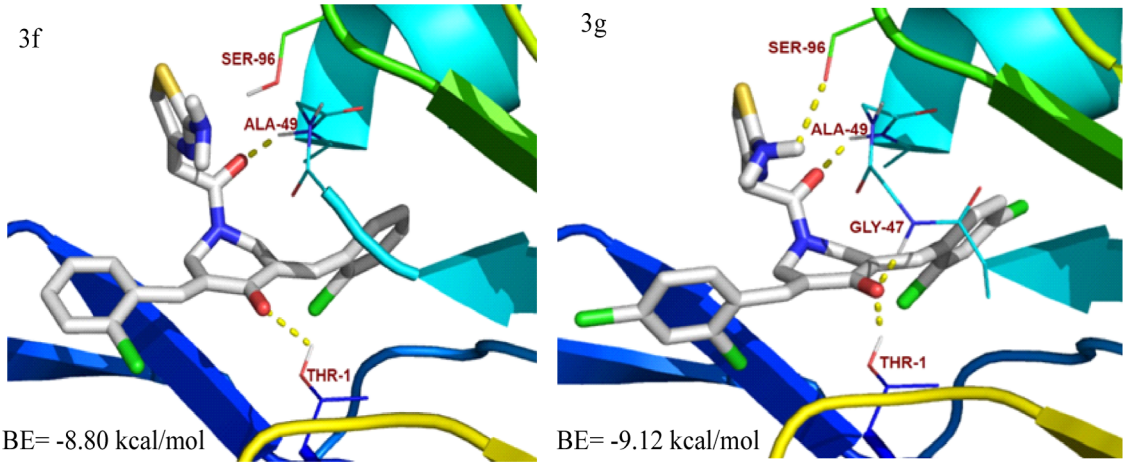

Figure 3. Model of predicted binding modes of compound 5f and 5g.

Table 4. Predicted Binding Free Energy (kcal/mol) of Compounds 5a−k with β5 Active Site of the 20S Proteasome

compound	binding energy (kcal/mol)	compound	binding energy (kcal/mol)
5a	−7.88	5g	−9.12
5b	−8.00	5h	−8.49
5c	−7.84	5i	−8.00
5d	−8.13	5j	−8.50
5e	−8.43	5k	−7.54
5f	−8.80		

Table 5. Anticancer Activity of Compounds (5a−k)

		HeLa (cervical)		HCT116 (colon)	
s. no.	compound	average GI_{50} (μM)	±SD	average GI_{50} (μM)	±SD
1	5a	0.28	0.04	0.23	0.00
2	5b	0.95	0.21	0.4	0.00
3	5c	0.36	0.20	0.21	0.00
4	5d	0.28	0.04	0.23	0.03
5	5e	0.25	0.07	0.285	0.11
6	5f	0.15	0.07	0.15	0.07
7	5g	0.25	0.07	0.23	0.00
8	5h	0.22	0.02	0.195	0.01
9	5i	0.30	0.01	0.275	0.06
10	5j	0.68	0.18	0.275	0.04
11	5k	5.50	0.00	4.5	0.71
12	Bortezomib	0.003		0.0008	

the origin of the tumor cell line, i.e., colon or cervical. 3,5-Bis(4-boronic acid-benzylidene)-1-methyl-piperidin-4-one (AM114) exhibited the growth inhibitory activity of the 20S proteasome with an IC_{50} value of 1.5 μM against HCT116 cells using MTT assay[11] and an IC_{50} value of 8 μM by XTT assay in HeLa cells.[12] In the present work, the reported synthesis of some new *N*-acryloyl group was intercalated with a secondary binding site to increase the potency of 2-amino thiazole-substituted derivatives of BAP to improve the anticancer properties of BAP. The presence of aryl ring in 1,5-diaryl-3-oxo-1,4-pentadienyl group is essential for anticancer activity **5a** (mean GI_{50} = 0.25 and 0.23 μM), whereas its replacement with thiophene ring **5k** (Figure 4) resulted in a drastic reduction in

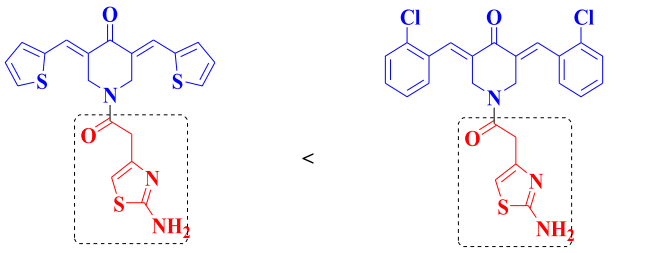

Figure 4. GI_{50} values of the thiophene and phenyl-substituted 1,5-diaryl-3-oxo-1,4-pentadienyl group.

activity (mean GI_{50} = 5 and 4.5 μM). The structure−activity relationship showed that the increase of the electronegativity of substituents (with monochloro or dichloro) in the aryl ring increased the cytotoxicity (mean GI_{50} range = ∼0.2 μM). The electron-releasing substituents on the aryl ring were found moderately to reduce the cytotoxicity potential, e.g., **5b** with O-Me substituent the mean GI_{50} = 0.675 μM, **5i** with thiomethyl ether substituent (GI_{50}= 0.3 and 0.275 μM), or **5j** with isopropyl substituent (GI_{50} = 0.47 and 0.275 μM). From Table 4, it was predicted by docking the presence of electronegative substituent in the aryl ring increasing the cytotoxicity. Compound **5f** was found to be most active in this series with a mean GI_{50} of 0.15 μM. The ubiquitin-mediated

https://doi.org/10.1021/acsomega.4c00039
ACS Omega 2024, 9, 29244−29251

protein degradation mechanism (proteasome inhibitor) is inhibited, and cervical cancer cells are preferred to be killed by BAP derivatives that have various amino acid substitutions on the amino group of 4-piperidone.[12] Significant cytotoxic effects can be achieved in cancer cells by inhibiting the cellular proteome, the rationale for developing these compounds as novel cancer chemotherapeutic agents.

3. EXPERIMENTAL SECTION

Materials and Methods. An open capillary tube method was used to determine the melting points using a Metler Toledo melting point apparatus, and they were uncorrected. Mass spectral data were recorded on an Agilent Technologies (LC/MSD VL) model: G1956A. The Bruker instrument was used to record ^{1}H and ^{13}C NMR spectra at 400 and 100 MHz, respectively, with TMS as an internal standard. Recording chemical shift values on the (δ) scale and measuring coupling constants (J) in hertz are done.

General Procedure: Synthesis of 3,5-Dibenzylidene-piperidin-4-one ***3(a−k)***. Benzaldehyde, **2** (5.2 g, 2.0 mmol), was added to a suspension of 4-piperidone hydrochloride monohydrate **1** (5.0 g, 1.0 mmol) in acetic acid (15 mL). Dry hydrogen chloride gas was passed through this mixture for 30 min at 0−5 °C. After being kept at room temperature for 12 h, the precipitate (AcOH salt of bischalcone) was poured into ice water, stirred for 15 min, filtered, washed with acetone, and dried (6.4 g) under vacuum.

Synthesis of 1-[2-(2-Amino-thiazol-4-yl)-acetyl]-3,5-dibenzylidene-piperidin-4-one ***5(a−k)***. The compound (**3a**) (2.0 g, 1.0 mmol) was dissolved in 10 mL of dichloro methane and cooled to 0−5 °C. Triethyl amine (2.2 g, 3.0 mmol) was added. (2-Amino-thiazol-4-yl)-acetyl chloride hydrochloride[41] (**4**) (2.3 g, 1.5 mmol) was slowly added and stirred for 30 min. Thin-layer chromatography (TLC) was checked, and the reaction was quenched in water (50 mL) and stirred for 10 min. The organic layer was dried with sodium sulfate. The organic layer was completely concentrated and dried to get the product 3.3 g (**5a**). To prove the generality of the reaction, the procedure was repeated with (**3b−k**) to get (**5b−k**).

1-[2-(2-Amino-thiazol-4-yl)-acetyl]-3,5-dibenzylidene-peridin-4-one ***(5a)***. Pale yellow solid, yellow solid, m.p: 184−186 °C; IR (KBr): ν 3388 (NH_2), 3118 (CH), 1651 (C═O), 1610 (amide C═O), 1251 (C−N) cm^{-1}; ^{1}H NMR (400 MHz, DMSO-d_6): δ 7.71 (s, 1H, CH), 7.64 (s, 1H, CH), 7.60−7.41 (m, 10H, Ar−H), 6.80 (br s, 2H, NH_2), 5.83 (s, 1H, thiazole CH), 4.88−4.83 (s, 4H, piperidone CH_2), 3.39 (s, 2H, CH_2); ^{13}C NMR (100 MHz, DMSO-d_6): δ 187.62, 186.05 (piperidone C═O), 168.19, 168.15 (amide C═O), 145.03, 136.15, 135.94, 134.88, 134.20, 133.75, 132.52, 130.57, 130.47, 130.41, 129.53, 129.02, 128.79, 128.64, 46.73, 42.52, 36.83; ESI-MS (m/z): 416.14 (M + H)$^+$, 417.14 (M + 2)$^+$; HRMS: 416.1426 (M + H)$^+$; $C_{24}H_{21}N_3O_2S$.

1-[2-(2-Amino-thiazol-5-yl)-acetyl]-3,5-bis(4-methoxy-benzylidene)-piperidin-4-one ***(5b)***. Yellow solid, mp: 178−180 °C; IR (KBr): ν 3348 (NH_2), 3140 (CH), 1649 (C═O), 1589 (amide C═O), 1251 (C−N) cm^{-1}; ^{1}H NMR(400 MHz, DMSO-d_6): δ 7.64 (s, 1H, CH), 7.58 (s, 1H, CH), 7.53−7.48 (m, 4H, AR-H), 7.07−7.05 (m, 4H, Ar−H), 6.81 (s, 2H, NH_2), 5.93 (s, 1H, thiazole CH), 4.86−4.80 (s, 4H, piperidone CH_2), 3.83 (s, 6H, CH_3), 3.41 (s, 2H, CH_2); ^{13}C NMR (100 MHz, DMSO-d_6): δ 190.94 (piperidone C═O), 173.37, 165.55 (amide C═O), 150.36, 141.05, 140.84, 137.88, 137.75, 135.76, 135.59, 132.21, 132.07, 119.62, 107.44, 60.58, 52.07, 47.78, 42.07; ESI-MS (m/z): 476.16 (M + H)$^+$; HRMS: 476.1639 (M + H)$^+$; $C_{26}H_{25}N_3O_4S$.

1-[2-(2-Amino-thiazol-5-yl)-acetyl]-3,5-bis(4-fluoro-benzylidene)-piperidin-4-one ***(5c)***. Pale yellow solid, m.p: 167−169 °C; IR (KBr): ν 3354, (NH_2), 3179 (CH), 1649 (C═O), 1597 (amide C═O), 1257 (C−N) cm^{-1}; ^{1}H NMR (400 MHz, DMSO-$d6$): δ 7.68 (s, 1H, CH), 7.65 (s, 1H, CH), 7.62−7.57 (m, 4H, Ar−H), 7.37−7.31 (m, 4H, Ar−H), 6.8 (s, 2H, NH_2), 5.89 (s, 1H, thiazole CH), 4.86−4.79 (s, 4H, piperidone CH_2), 3.41 (s, 2H, CH_2); ^{13}C NMR (100 MHz, $CDCl_3$): δ 185.93 (piperidone C═O), 168.20 (amide C═O), 163.75, 161.28, (J_{CF} = 247 Hz) 145.02, 134.97, 134.81, 133.02, 132.89, 132.80, 132.31, 132.21, 130.94, 130.75, 115.95, 115.73, 102.16, 46.67, 42.35, 36.85; ESI-MS (m/z): 452.12 (M + H)$^+$; HRMS: 452.1253 (M + H)$^+$; $C_{24}H_{19}F_2N_3O_2S$.

1-[2-(2-Amino-thiazol-5-yl)-acetyl]-3,5-bis(2-fluoro-benzylidene)-piperidin-4-one ***(5d)***. Yellow solid, m.p: 168−170 °C; IR (KBr): ν 3334 (NH_2), 3115 (CH), 1660 (C═O), 1610 (amide C═O), 1247 (C−N) cm^{-1}; ^{1}H NMR (400 MHz, $CDCl_3$): δ 7.91 (s, 1H, CH), 7.83 (s, 1H, CH), 7.44−7.12 (m, 8H, Ar−H), 5.82 (s, 1H, thiazole CH), 5.17 (s, 2H, NH_2), 4.80−4.66 (s, 4H, piperidone CH_2), 3.46 (s, 2H, CH_2); ^{13}C NMR (100 MHz, $CDCl_3$): δ 185.89 (piperidone C═O), 168.61, 167.90 (amide C═O), 162.27, 159.47, (J_{CF} = 280 Hz) 144.80, 133.46, 133.20, 131.54, 131.46, 131.38, 131.22, 130.85, 130.81,130.06, 124.28,122.70, 122.57, 122.44, 116.32, 116.10, 115.88, 104.49, 47.16, 43.68, 37.38; ESI-MS (m/z): 452.2 (M + H)$^+$; HRMS: 452.1253 (M + H)$^+$; $C_{24}H_{19}F_2N_3O_2S$.

1-[2-(2-Amino-thiazol-5-yl)-acetyl]-3,5-bis(4-chloro-benzylidene)-piperidin-4-one ***(5e)***. Pale yellow solid, m.p: 178−180 °C; IR (KBr): ν 3305 (NH_2), 1651 (C═O), 1600 (amide C═O), 1253 (C−N) cm^{-1}; ^{1}H NMR (400 MHz, $CDCl_3$): δ 7.76 (s, 1H, CH), 7.72 (s, 1H, CH), 7.44−7.30 (m, 8H, Ar−H), 6.01 (s, 1H, thiazole CH), 4.88 (s, 2H, NH_2), 4.78 (s, 4H, piperidone CH_2), 3.54 (s, 2H, CH_2); ^{13}C NMR (100 MHz, DMSO-d_6): δ 185.85 (piperidone C═O), 171.65, 168.23, 168.06 (amide C═O), 145.00, 144.90, 134.83, 134.66, 134.23, 133.19, 133.04, 132.32, 132.18, 128.83, 102.82, 102.19, 100.33, 46.72, 42.36,37.09, 36.83, 30.67; ESI-MS (m/z): 484.1 (M + H)$^+$, 485.1 (M + 2)$^+$; HRMS: 484.0636 (M + H)$^+$; $C_{24}H_{19}Cl_2N_3O_2S$.

1-[2-(2-Amino-thiazol-5-yl)-acetyl]-3,5-bis(2-chloro-benzylidene)-piperidin-4-one ***(5f)***. Pale yellow solid, m.p 196−198 °C; IR (KBr): ν 3373 (NH_2), 3124 (CH), 1654 (C═O), 1608 (amide C═O), 1246 (C−N) cm^{-1}; ^{1}H NMR (400 MHz, $CDCl_3$): δ 8.00 (s, 1H, CH), 7.96 (s, 1H, CH), 7.50−7.19 (m, 8H, Ar−H), 5.83 (s, 1H, thiazole CH), 5.05 (s, 2H, NH_2), 4.76−4.63 (s, 4H, piperidone CH_2), 3.43 (s, 2H, CH_2); ^{13}C NMR (100 MHz, DMSO-d_6): δ 185.80 (piperidone C═O), 168.23, 168.17 (amide C═O), 144.88, 134.06, 134.00, 133.87, 132.75, 132.55, 132.11, 131.16, 130.91, 129.85, 127.40, 101.99, 79.15, 46.26, 42.31, 40.13, 39.92, 36.76; ESI-MS (m/z): 484.0 (M + H)$^+$, 485.0 (M + 2)$^+$; HRMS: 484.0651 (M + H)$^+$; $C_{24}H_{19}Cl_2N_3O_2S$.

1-[2-(2-Amino-thiazol-5-yl)-acetyl]-3,5-bis(2,4-dichloro-benzylidene)-piperidin-4-one ***(5g)***. Pale yellow solid, m.p: 165−167 °C; IR (KBr): ν 3379 (NH_2), 3132 (CH), 1653 (C═O), 1620 (amide C═O), 1251 (C−N) cm^{-1}; ^{1}H NMR (400 MHz, DMSO-d_6): δ 7.80−7.79 (s, 2H, CH), 7.75−7.49 (m, 6H, Ar−H), 6.80 (s, 2H, NH_2), 5.85 (s, 1H, thiazole CH), 4.74−4.67 (s, 4H, piperidone CH_2), 3.36 (s, 2H, CH_2); ^{13}C NMR (100 MHz, DMSO-d_6): δ 185.58 (piperidone C═O), 171.62, 168.27, 168.25, 168.05 (amide C═O), 144.90, 135.10,

https://doi.org/10.1021/acsomega.4c00039
ACS Omega 2024, 9, 29244−29251

134.85, 134.39, 132.00, 131.59, 131.22, 129.44, 127.62, 102.81, 102.06, 46.28, 42.17, 37.10, 36.74; ESI-MS (m/z): 554.1 $(M + H)^+$, 555.9 $(M + 2)^+$; HRMS: 553.9840 $(M + H)^+$; $C_{24}H_{17}Cl_4N_3O_2S$.

*1-[2-(2-Amino-thiazol-5-yl)-acetyl]-3,5-bis(3,4-dichloro-benzylidene)-piperidin-4-one (**5h**).* Yellow solid, m.p: 174−176 °C; IR (KBr): ν 3373 (NH_2), 3118 (CH), 1664 (C═O), 1608 (amide C═O), 1251 (C−N) cm^{-1}; ^1H NMR (400 MHz, DMSO-d_6): 7.86 (s, 1H, CH), 7.79 (s, 1H, CH), 7.77−7.73 (m, 2H, Ar−H), 7.64−7.47 (m, 4H, Ar−H), 6.78 (s, 2H, NH_2), 5.92 (s, 1H, thiazole CH), 4.85−4.77 (s, 4H, piperidone CH_2), 3.44 (s, 2H, CH_2); ^{13}C NMR (100 MHz, DMSO-d_6): δ 185.71(piperidone C═O), 168.30, 168.27 (amide C═O), 145.04, 134.99, 134.82, 134.03, 133.96, 133.63, 132.28, 132.05, 131.52, 130.81, 130.27, 102.13, 46.65, 42.20, 36.94; ESI-MS (m/z): 552.0 $(M + H)^+$, 554.0 $(M + 3)^+$; HRMS: 553.9840 $(M + H)^+$; $C_{24}H_{17}Cl_4N_3O_2S$.

*1-[2-(2-Amino-thiazol-5-yl)-acetyl]-3,5-bis(4-methylsulfanyl-benzylidene)-piperidin-4-one (**5i**).* Yellow solid, m.p: 175−177 °C; IR (KBr): ν 3346 (NH_2), 3124 (CH), 1651 (C═O), 1610 (amide C═O), 1253 (C−N) cm^{-1}; ^1H NMR (400 MHz, DMSO-d_6): δ 7.64 (s, 1H, CH), 7.57 (s, 1H, CH), 7.50−7.42 (m, 4H, Ar−H), 7.36−7.33 (m, 4H, Ar−H), 6.80 (s, 2H, NH_2), 5.92 (s, 1H, thiazole CH), 4.86−4.80 (s, 4H, piperidone CH_2), 3.32(s, 2H, CH_2), 2.53−2.50 (s, 6H, CH_3); ^{13}C NMR (100 MHz, DMSO-d_6): δ 185.7 (piperidone C═O), 168.20, 168.16 (amide C═O), 145.07, 140.93, 135.59, 135.40, 131.82, 131.66, 131.17, 131.03, 130.65, 125.47, 102.23, 46.87, 42.51, 36.82, 14.13; ESI-MS (m/z): 508.1 $(M + H)^+$, 509.2 $(M + 2)^+$; HRMS: 508.1181 $(M + H)^+$; $C_{26}H_{25}N_3O_2S_3$.

*1-[2-(2-Amino-thiazol-5-yl)-acetyl]-3,5-bis(4-isopropyl-benzylidene)-piperidin-4-one (**5j**).* Yellow solid, m.p: 188−190 °C; IR (KBr): ν 3365 (NH_2), 3111 (CH), 1656 (C═O), 1606 (amide C═O), 1249 (C−N) cm^{-1}; ^1H NMR (400 MHz, $CDCl_3$): δ 7.79 (s, 2H, CH), 7.42−7.26 (m, 8H, Ar−H), 5.79 (s, 1H, thiazole CH), 5.23 (s, 2H, NH_2), 4.93−4.78 (s, 4H, piperidone CH_2), 3.49 (s, 2H, CH_2), 2.99−2.90 (m, 2H, CH), 1.27 (m, 12H, CH_3); ^{13}C NMR (100 MHz, $CDCl_3$): δ 186.6 (piperidone C═O), 168.62, 168.01(amide C═O), 150.82, 144.94, 138.39, 137.07, 132.32, 132.24, 131.10, 130.93, 130.66, 126.95, 126.91, 104.48, 46.98, 43.86, 37.58, 34.09, 23.84, 23.79; ESI-MS (m/z): 500.4 $(M + H)^+$, 501.4 $(M + 2)^+$; HRMS: 500.2366 $(M + H)^+$; $C_{30}H_{33}N_3O_2S$.

*1-[2-(2-Amino-thiazol-5-yl)-acetyl]-3,5-bis-thiophen-2-yl-methylene-piperidin-4-one (**5k**).* Pale yellow solid, m.p: 219−221 °C; ^1H NMR (400 MHz, DMSO-d_6): δ 7.96−7.95 (s, 2H, CH), 7.88−7.27 (m, 6H, thiophene CH), 6.81 (s, 2H, NH_2), 6.14 (s, 1H, thiazole CH), 4.87 (s, 4H, piperidone CH_2), 3.58 (s, 2H, CH_2); ^{13}C NMR (100 MHz, DMSO-d_6): δ 184.71 (piperidone C═O), 168.32, 168.23 (amide C═O), 145.00, 137.58, 137.51, 134.65, 134.36, 132.42, 132.32, 129.15, 128.89, 128.62, 128.48, 128.41, 128.06, 102.38, 67.00, 46.60, 42.22, 36.85; ESI-MS (m/z): 428.1 $(M + H)^+$; HRMS: 428.0554 $(M + H)^+$; $C_{20}H_{17}N_3O_2S_3$.

*Crystallography Data (**5c**).* The X-ray diffraction quality crystals of compound **5c** were obtained by slow evaporation of methanol. A suitable crystal was mounted on a Nylon loop and placed on an Agilent Gemini, EOS, single-crystal X-ray diffractometer. The crystal was kept at 173(2) K during data collection. Using the Olex2 software package, the structure was solved with Superflip using Charge Flipping and refined with the ShelXL refinement package using least-squares minimization refinement on F^2. Hydrogen atoms were included in the refinement as per the riding model. All of the remaining crystal parameters are represented in Table 2.

Docking Simulation. Geometries of compounds **5(a−k)** have been fully optimized using hybrid density functional theory (B3LYP). The 6-31G* basis set was used to describe all atoms. Vibrational frequency calculations were performed on these optimized structures to confirm minimum energy geometries by observing all positive frequencies. All of these computations were carried out using the Gaussian 09 program.[39] We used these optimized geometries for docking simulation. The docking simulation studies were performed with AutoDock 4.2,[40] and the figures were generated using PyMOL 1.3. From the RCSB Data Bank, the recently solved 20S proteasome (PDB ID: 4NO8)[42] crystal structure has been retrieved and all heteroatoms were removed. We have selected the β5 (K chain) for docking simulation because the K chain is responsible for the chymotrypsin-like (ChT-L) activities. The standard parameters were adapted for the docking studies as stated in the AutoDock user guide, except for the following modifications stated below. The grid box was prepared as a 40 × 40 × 40 Å box with a spacing of 0.375, positioned in the ligand value (11.667−137.254 14.834). Lamarckian genetic algorithm (LGA) was used to carry out the ligand−protein interactions. The population size was 150, the maximum number of energy evaluations was 2 500 000 based on the number of rotatable bonds, the maximum number of generations was retained in 27000, and the number of GAruns was 10. The docked free energy was adopted in this analysis.

Cytotoxicity Assay. The cytotoxicity assay procedure (S29) and raw data on anticancer activity for compounds **5(a−k)** (Table S1) are available in the Supporting Information.

CONCLUSIONS

In silico docking studies revealed a favorable interaction of the chlorine atom in the aryl ring of **5e−5h** with the catalytic site of the 20S proteasome, which can be achieved through the N-terminal threonine residue of the β-subunits to the carbonyl group of 3,5-bis(arylidene)-4-piperidones compounds. The piperidone ring's C═O group (**5g**) interacts with hydrogen bonding, the HO group of the THR-1 (Threonine) residue, and the NH group of the GLY-47 (Glycine) residue. An additional C═O group of amide interacted with the NH group of the ALA-49 (Alanine) residue, and the NH group of amino thiazole contacted with the OH group of SER-96 (serine) residue. The amino thiazole interacted with the OH group of SER-96 (serine) residue of the 20S proteasome. The synthesized chalcones **5a−5j** were found to have GI_{50} values in the range of 0.15−0.28 μM toward HeLa cell and HCT116 cancer cell lines. The replacement of the phenyl ring with a thiophene ring in **3k** was found to have GI_{50} > 4 μM in both cell lines. The compounds (**5e−5h**) showed most potent cytotoxic activity (Mean GI_{50}= 0.15−0.25 and 0.15−0.28 μM) toward the tested HeLa cell and HCT116 cancer cell lines and the docking binding energy −8.43 to −9.2 (kcal/mol).

ASSOCIATED CONTENT

Supporting Information

The Supporting Information is available free of charge at https://pubs.acs.org/doi/10.1021/acsomega.4c00039.

^1H, ^{13}C NMR, mass, HRMS, and FT-IR data for compounds **5(a−k)**, cytotoxicity assay, and raw data anticancer activity for compounds **5(a−k)** (PDF)

https://doi.org/10.1021/acsomega.4c00039
ACS Omega 2024, 9, 29244−29251

AUTHOR INFORMATION

Corresponding Author

Sundaramoorthy Sarveswari − *Department of Chemistry, School of Advanced Sciences, VIT University, Vellore 632014 Tamil Nadu, India;* orcid.org/0000-0003-2469-0678; Phone: +91-416-2202535; Email: ssarveswari@vit.ac.in, sarveswari@gmail.com; Fax: +91-4162203092

Authors

Thangaiyan Suresh − *Department of Chemistry, School of Advanced Sciences, VIT University, Vellore 632014 Tamil Nadu, India*

Dhatchana Moorthy Nachiappan − *Department of Biochemistry, University of Madras, Chennai 600025 Tamil Nadu, India;* Present Address: R&D- AI, EinNext Biosciences, No. 2, Gowrivakkam, Chennai 600 073, Tamil Nadu, India; orcid.org/0000-0002-0071-4762

G. Karthikeyan − *Amity Institute of Virology and Immunology, Amity University, Noida 201303 Uttar Pradesh, India*

Vijayaparthasarathi Vijayakumar − *Department of Chemistry, School of Advanced Sciences, VIT University, Vellore 632014 Tamil Nadu, India;* orcid.org/0000-0002-0744-7986

Jerry P Jasinski − *Keene State College, Keene, New Hampshire 03435-200, United States*

Complete contact information is available at: https://pubs.acs.org/10.1021/acsomega.4c00039

Notes

The authors declare no competing financial interest.

ACKNOWLEDGMENTS

T.S. was thankful to VIT University for providing facility. S.S. is thankfull to VIT seed grant SG20230087 and VIT SIF for providing NMR facilty.

REFERENCES

(1) ME, J. F.; Siegel, R. L.; Isabelle Soerjomataram, M. D.; Ahmedin Jemal, D. V. M. Global cancer statistics 2022: GLOBOCAN estimates of incidence and mortality worldwide for 36 cancers in 185 countries. 2024.

(2) Chen, Z. J. Ubiquitin signalling in the NF-κB pathway. *Nat. Cell Biol.* **2005**, *7*, 758−765.

(3) Fricker, L. D. Proteasome Inhibitor Drugs. *Annu. Rev. Pharmacol. Toxicol.* **2020**, *60*, 457−476.

(4) Reed, S. I. The ubiquitin-proteasome pathway in cell cycle control. In *Cell Cycle Regulation*; Springer, 2006; pp 147−181.

(5) Huen, M. S.; Chen, J. The DNA damage response pathways: at the crossroad of protein modifications. *Cell Res.* **2008**, *18*, 8−16.

(6) Kostova, Z.; Tsai, Y. C.; Weissman, A. M. Ubiquitin ligases, critical mediators of endoplasmic reticulum-associated degradation. *Semin. Cell Dev. Biol.* **2007**, *18* (6), 770−779.

(7) Wang, J.; Maldonado, M. A. The ubiquitin-proteasome system and its role in inflammatory and autoimmune diseases. *Cell Mol. Immunol.* **2006**, *3* (4), 255−261.

(8) Hoeller, D.; Hecker, C. M.; Dikic, I. Ubiquitin and ubiquitin-like proteins in cancer pathogenesis. *Nat. Rev. Cancer* **2006**, *6*, 776−788.

(9) Ramsewak, R.; DeWitt, D.; Nair, M. G. Cytotoxicity, antioxidant and anti-inflammatory activities of curcumins I−III from *Curcuma longa*. *Phytomedicine* **2000**, *7*, 303−308.

(10) Milacic, V.; Banerjee, S.; Landis-Piwowar, K. R.; Sarkar, F. H.; Majumdar, A. P.; Dou, Q. P. Curcumin inhibits the proteasome activity in human colon cancer cells in vitro and in vivo. *Cancer Res.* **2008**, *68* (18), 7283−7292.

(11) Achanta, G.; Modzelewska, A.; Feng, L.; Khan, S. R.; Huang, P. A boronic-chalcone derivative exhibits potent anticancer activity through inhibition of the proteasome. *Mol. Pharmacol.* **2006**, *70* (1), 426−433.

(12) Bazzaro, M.; Anchoori, R. K.; Mudiam, M. K. R.; Issaenko, O.; Kumar, S.; Karanam, B.; Khan, S. R.; et al. α, β-Unsaturated carbonyl system of chalcone-based derivatives is responsible for broad inhibition of proteasomal activity and preferential killing of human papilloma virus (HPV) positive cervical cancer cells. *J. Med. Chem.* **2011**, *54* (2), 449−456.

(13) Ahsan, M. J.; Saini, D.; Sharma, P.; Jadav, S. S.; Bakht, M. A.; Salahuddin; Alluri, R.; Faiyazuddin, M. Synthesis, Biological Evaluation and Molecular Docking Studies Against EGFR Tyrosine Kinase of 3,5-bis (substituted benzylidene)-1-ethylpiperidin-4-one Analogues. *Lett. Org. Chem.* **2021**, *18* (9), 710−720.

(14) Kisselev, A. F. A novel bullet hits the proteasome. *Cancer Cell* **2013**, *24*, 691−693.

(15) Dimmock, J. R.; Arora, V. K.; Duffy, M. J.; Reid, R. S.; Allen, T. M.; Kao, G. Y. Evaluation of some N-acyl analogues of 3, 5-bis (arylidene)-4-piperidones for cytotoxic activity. *Drug Des. Discovery* **1992**, *8*, 291−299.

(16) Dimmock, J. R.; Padmanilayam, M. P.; Puthucode, R. N.; Nazarali, A. J.; Motaganahalli, N. L.; Zello, G. A.; Quail, J. W.; Oloo, E. O.; Kraatz, H. B.; Prisciak, J. S.; Allen, T. M.; Santos, C. L.; Balzarini, J.; De Clercq, E.; Manavathu, E. K. A conformational and structure-activity relationship study of cytotoxic 3, 5-bis (arylidene)-4-piperidones and related N-acryloyl analogues. *J. Med. Chem.* **2001**, *44*, 586−593.

(17) Sun, A.; Lu, Y. J.; Hu, H.; Shoji, M.; Liotta, D. C.; Snyder, J. P. Curcumin analog cytotoxicity against breast cancer cells: exploitation of a redox-dependent mechanism. *Bioorg. Med. Chem. Lett.* **2009**, *19* (23), 6627−6631.

(18) Selvendiran, K.; Tong, L.; Bratasz, A.; Kuppusamy, M. L.; Ahmed, S.; Ravi, Y.; Trigg, N. J.; Rivera, B. K.; Kálai, T.; Hideg, K.; Kuppusamy, P. Anticancer efficacy of a difluorodiarylidenyl piperidone (HO-3867) in human ovarian cancer cells and tumor xenografts. *Mol. Cancer Ther.* **2010**, *9*, 1169−1179.

(19) Ayati, A.; Saeed, E.; Ali, A.; Abbas, S.; Alireza, F. Recent applications of 1,3-thiazole core structure in the identification of new lead compounds and drug discovery. *Eur. J. Med. Chem.* **2015**, *97*, 699−718.

(20) Sharma, P. C.; Bansal, K. K.; Sharma, A.; Sharma, D.; Deep, A. Thiazole-containing compounds as therapeutic targets for cancer therapy. *Eur. J. Med. Chem.* **2020**, *188*, No. 112016.

(21) Morigi, R.; Locatelli, A.; Leoni, A.; Rambaldi, M. Recent patents on thiazole derivatives endowed with antitumor activity. *Recent Pat. Anti-cancer Drug Discovery* **2015**, *10* (3), 280−297.

(22) Altıntop, M. D.; Özdemir, A.; Turan-Zitouni, G.; Ilgın, S.; Atlı, Ö.; Demirci, F.; Kaplancıklı, Z. A. Synthesis and in vitro evaluation of new nitro-substituted thiazolyl hydrazone derivatives as anticandidal and anticancer agents. *Molecules* **2014**, *19* (9), 14809−14820.

(23) Farghaly, T. A.; Abbas, E. M.; Al-Soliemy, A. M.; Sabour, R.; Shaaban, M. R. Novel sulfonyl thiazolyl-hydrazone derivatives as EGFR inhibitors: Design, synthesis, biological evaluation and molecular docking studies. *Bioorg. Chem.* **2022**, *121*, No. 105684.

(24) Aljohani, G. F.; Abolibda, T. Z.; Alhilal, M.; Al-Humaidi, J. Y.; Alhilal, S.; Ahmed, H. A.; Gomha, S. M. Novel thiadiazole-thiazole hybrids: Synthesis, molecular docking, and cytotoxicity evaluation against liver cancer cell lines. *J. Taibah Univ. Sci.* **2022**, *16* (1), 1005−1015.

(25) Ayman, M.; Gomha, S. M.; Abdallah, M. A.; ElNashar, d.; Soliman, A. M.; Rashdan, H. R. In Sight into innovative cancer therapeutic approach based on nanotechnology: Chitosan (CS)/Polyvinyl alcohol (PVA) films loaded with synthesized bisthiazole derivative for cancer treatment. *Egypt. J. Chem.* **2023**, *66* (13), 1997−2011.

(26) Hussein, A. M.; Gomha, S. M.; El-Ghany, N. A. A.; Zaki, M. E.; Farag, B.; Al-Hussain, S. A.; Mohamed, N. A.; et al. Green Biocatalyst for Ultrasound-Assisted Thiazole Derivatives: Synthesis, Antibacterial

Evaluation, and Docking Analysis. *ACS Omega* **2024**, *9*, 13666−13679.
(27) Al-Humaidi, J. Y.; Gomha, S. M.; Riyadh, S. M.; Ibrahim, M. S.; Zaki, M. E.; Abolibda, T. Z.; Jefri, O. A.; Abouzied, A. S. Synthesis, biological evaluation, and molecular docking of novel azolylhydrazonothiazoles as potential anticancer agents. *ACS Omega* **2023**, *8* (37), 34044−34058.
(28) Kassab, R. M.; Al-Hussain, S. A.; Abdelmonsef, A. H.; Zaki, M. E.; Gomha, S. M.; Muhammad, Z. A. Novel xylenyl-spaced bis-thiazoles/thiazines: synthesis, biological profile as herpes simplex virus type 1 inhibitors and in silico simulations. *Future Med. Chem.* **2024**, *16* (1), 27−41.
(29) Sayed, A. R.; Elsawy, H.; Shaaban, S.; Gomha, S. M.; Al-Faiyz, Y. S. Design, Synthesis, and Biological Evaluations of Novel Azothiazoles Based on Thioamide. *Curr. Issues Mol. Biol.* **2022**, *44* (7), 2956−2966.
(30) Abdallah, A. M.; Gomha, S. M.; Zaki, M. E.; Abolibda, T. Z.; Kheder, N. A. A green synthesis, DFT calculations, and molecular docking study of some new indeno [2, 1-b] quinoxalines containing thiazole moiety. *J. Mol. Struct.* **2023**, *1292*, No. 136044.
(31) Orujova, T.; Ece, A.; Akalın Çiftçi, G.; Özdemir, A.; Altıntop, M. D. A new series of thiazole-hydrazone hybrids for Akt-targeted therapy of non-small cell lung cancer. *Drug Dev. Res.* **2023**, *84* (2), 185−199.
(32) Borelli, C.; Schaller, M.; Niewerth, M.; Nocker, K.; Baasner, B.; Berg, D.; Tiemann, R.; Tietjen, K.; Fugmann, B.; Lang-Fugmann, S.; Korting, H. C. Modes of action of the new arylguanidine abafungin beyond interference with ergosterol biosynthesis and in vitro activity against medically important fungi. *Chemotherapy* **2008**, *54*, 245−259.
(33) Al-Balas, Q.; Anthony, N. G.; Al-Jaidi, B.; Alnimr, A.; Abbott, G.; Brown, A. K.; Taylor, R. C.; Besra, G. S.; McHugh, T. D.; Gillespie, S. H.; Johnston, B. F.; Mackay, S. P.; Coxon, G. D. Identification of 2-aminothiazole-4-carboxylate derivatives active against Mycobacterium tuberculosis H37Rv and the beta-ketoacyl-ACP synthase mtFabH. *PLoS One* **2009**, *4*, No. e5617.
(34) Bell, F. W.; Cantrell, A. S.; Hoegberg, M.; Jaskunas, S. R.; Johansson, N. G.; Jordan, C. L.; Kinnick, M. D.; Lind, P.; Morin, J. M., Jr. Phenethylthiazolethiourea (PETT) Compounds, a New Class of HIV-1 Reverse Transcriptase Inhibitors. 1. Synthesis and Basic Structure-Activity Relationship Studies of PETT Analogs. *J. Med. Chem.* **1995**, *38* (25), 4929−4936.
(35) Hassan, G. S.; El-Messery, S. M.; Al-Omary, F. A.; El-Subbagh, H. I. Substituted thiazoles VII. Synthesis and antitumor activity of certain 2-(substituted amino)-4-phenyl-1, 3-thiazole analogs. *Bioorg. Med. Chem. Lett.* **2012**, *22* (20), 6318−6323.
(36) Hussein, A. H. M.; Khames, A. A.; El-Adasy, A. B. A.; Atalla, A. A.; Abdel-Rady, M.; Hassan, M. I.; Nemr, M. T. M.; Elshaier, Y. A. Design, synthesis and biological evaluation of new 2-aminothiazole scaffolds as phosphodiesterase type 5 regulators and COX-1/COX-2 inhibitors. *RSC Adv.* **2020**, *10* (50), 29723−29736.
(37) Alizadeh, S. R.; Hashemi, S. M. Development and therapeutic potential of 2-aminothiazole derivatives in anticancer drug discovery. *Med. Chem. Res.* **2021**, *30*, 771−806.
(38) Guedes, R. A.; Serra, P.; Salvador, J. A.; Guedes, R. C. Computational approaches for the discovery of human proteasome inhibitors: An overview. *Molecules* **2016**, *21* (7), 927.
(39) Frisch, M. J.; Trucks, G. W.; Schlegel, H. B.; Scuseria, G. E.; Robb, M. A.; Cheeseman, J. R.; Scalmani, G.; Barone, V.; Mennucci, B.; Petersson, G. A.; Nakatsuji, H.; Caricato, M.; Li, X.; Hratchian, H. P.; Izmaylov, A. F.; Bloino, J.; Zheng, G.; Sonnenberg, J. L.; Hada, M.; Ehara, M.; Toyota, K.; Fukuda, R.; Hasegawa, J.; Ishida, M.; Nakajima, T.; Honda, Y.; Kitao, O.; Nakai, H.; Vreven, T.; Montgomery, J. A., Jr.; Peralta, J. E.; Ogliaro, F.; Bearpark, M.; Heyd, J. J.; Brothers, E.; Kudin, K. N.; Staroverov, V. N.; Kobayashi, R.; Normand, J.; Raghavachari, K.; Rendell, A.; Burant, J. C.; Iyengar, S. S.; Tomasi, J.; Cossi, M.; Rega, N.; Millam, J. M.; Klene, M.; Knox, J. E.; Cross, J. B.; Bakken, V.; Adamo, C.; Jaramillo, J.; Gomperts, R.; Stratmann, R. E.; Yazyev, O.; Austin, A. J.; Cammi, R.; Pomelli, C.; Ochterski, J. W.; Martin, R. L.; Morokuma, K.; Zakrzewski, V. G.; Voth, G. A.; Salvador, P.; Dannenberg, J. J.; Dapprich, S.; Daniels, A. D.; Farkas, O.; Foresman, J. B.; Ortiz, J. V.; Cioslowski, J.; Fox, D. J. *Gaussian 09*, Revision D.01, Gaussian, Inc.: Wallingford CT, 2009.
(40) Garrett, M. M.; Goodsell, D. S.; Pique, M. E.; William "Lindy" Lindstrom, R. H.; Stefano Forli, E. H.; Forli, S. H.; Belew, R.; Olson, A. J. *AutoDock Version 4.2*.
(41) Imada, A.; Hirai, S. Cefotiam hexetil. *Int. J. Antimicrob. Agents* **1995**, *5* (2), 85−99.
(42) Stein, M. L.; Cui, H.; Beck, P.; Dubiella, C.; Voss, C.; Krüger, A.; Schmidt, B.; Groll, M. Systematic comparison of peptidic proteasome inhibitors highlights the α-ketoamide electrophile as an auspicious reversible lead motif. *Angew. Chem., Int. Ed.* **2014**, *53* (6), 1679−1683.

https://doi.org/10.1021/acsomega.4c00039
ACS Omega 2024, 9, 29244−29251